Zeitschrift: Schweizerische mineralogische und petrographische Mitteilungen = Bulletin suisse de minéralogie et pétrographie

Band: 68 (1988)

Heft: 2

Artikel: OH-rich topaz from alpine fissures in triassic dolomites near Lugnez, Graubünden (mesozoic cover of Gotthard Massif, Swiss Alps)

Autor: Soom, M. / Armbruster, Th. / Stalder, H.A.

DOI: https://doi.org/10.5169/seals-52056

SCHWEIZ. MINERAL. PETROGR. MITT. 68, 141-155, 1988

OH-rich Topaz from Alpine Fissures in Triassic Dolomites near Lugnez, Graubünden (Mesozoic Cover of Gotthard Massif, Swiss Alps).

by *M. Soom*[1], *Th. Armbruster*[2] and *H.A. Stalder*[1]

Abstract

An Alpine fissure topaz, occuring together with quartz and dickite in Triassic dolomites near Lugnez, Graubünden (Switzerland) is described. Optical data and cell dimensions were determined for one selected single crystal which was previously heated at 950 °C yielding: $\alpha = 1.624$, $\gamma = 1.637$, $2V_z = 53°$, a = 4.6548(8) Å, b = 8.820(2) Å, c = 8.380(2) Å, a∥X, b∥Y, c∥Z. Without heating topaz shows characteristic sector zoning. OH-F substitution was estimated from cell dimensions and optical data leading to molar F/(F+OH)-values between 0.75 and 0.85. Fluid inclusion measurements in syngenetic quartz indicate that topaz grew in NaCl-bearing, high CO_2 hydrothermal solutions at temperatures above 250 °C and pressures around 2.5-3.0 kbar. Towards the end of mineralization occurred CO_2-water unmixing, liberating a CO_2-rich vapour phase which favoured the precipitation of carbonates and sulfides.

Keywords: Topaz, Alpine fissures, fluid inclusions, substitution, dolomite, Grisons, Switzerland

1. Introduction

In 1983 an amateur-mineralogist (H. Luginbühl, Windisch) discovered in quartz-bearing fissures in the Lugnez area several prismatic crystals which were determined as topaz (H.A.St.). This mineral has been described in the Alps from hercynic, turmalin-pegmatites in the Lötschental (TRUNINGER, 1911 a+b) and from kyanite-quartz-schists and pegmatites in the Untersulzbachtal (MEIXNER, 1978). Thus topaz from Lugnez can be considered as the first occurrence of this mineral in Tertiary Alpine fissures.

The simplified formula of topaz is Al_2 (F, OH) [SiO_4]. In natural topaz up to 30 mol% OH may substitute for F, which affects optical properties and lattice parameters (RIBBE, 1982).

2. Geological Setting

The topaz-bearing fissures are situated in the lower part of Val Renastga, Lugnez GR (coordinates deposited at the Museum of Natural History, Berne). This region is located on the southern border of the sedimentary cover of the Gotthard massif and close to the thrust fault of the Pennine nappes. The mesozoic metasediments consist of Triassic quartzites, phyllites, rauhwacke, dolomites, gypsum and Liassic calcareous phyllites. The mineral bearing fissures are restricted to a strongly tectonized dolomite layer, approximately 100-200 m below the thrustzone of the Pennine nappes, with boudinage structure and a thickness of several meters. This layer is situated at the basis of a normal serie of Triassic and Liassic metasediments which are considered as imbricated mesozoic cover of the Gotthard massif ("Peidener Schuppenzone", in NABHOLZ and VOLL, 1963 or "Pianca-Zone" in JUNG, 1963). The mesozoic metasediments show a complex Alpine deformation history which can be subdivided into several phases of folding. In the outcrop the following structures according to NABHOLZ and VOLL (1963) can be observed: bedding S_0,

[1] Naturhistorisches Museum, Bernastr. 15, CH-3005 Bern.
[2] Laboratorium für chemische und mineralogische Kristallographie, Universität Bern, Freiestr. 3, CH-3012 Bern.

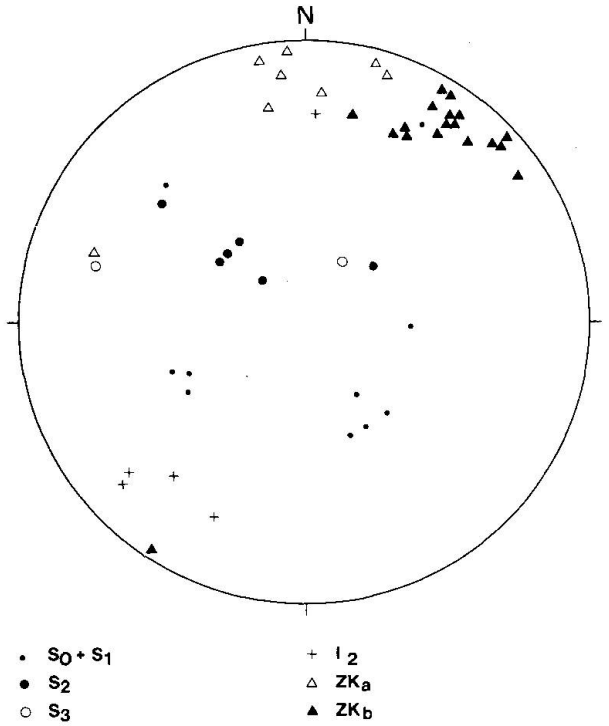

Fig. 1a Stereogram of structures in Val Renastga, Lugnez (Schmidt net, lower hemisphere): S_0bedding, S_2 main schistosity, l_2 stretching lineation, S_3 crenulation cleavage, ZK_a veins filled with quartz and carbonates, ZK_b topaz-bearing fissures.

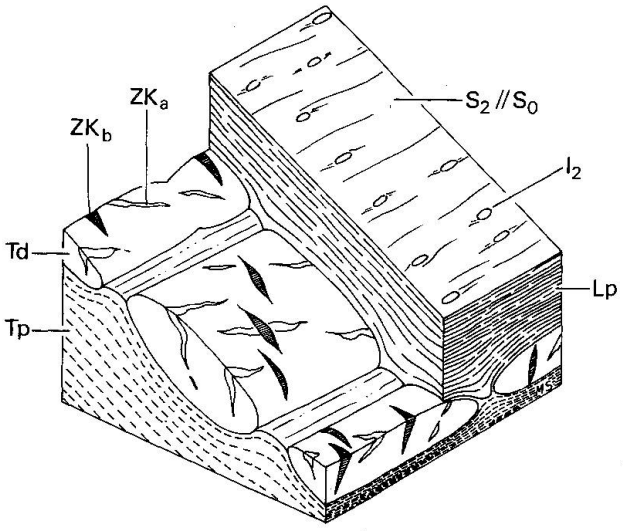

Fig. 1b Sketch diagram, topaz locality Lugnez. Tp Triassic phyllites, Td Triassic dolomites, Lp Liassic phyllites.

main schistosity S_2 subparallel to bedding with stretching lineation l_2, crenulation cleavage S_3 and related folds. Some structural measurements are summarized in Fig. 1 a+b.

The examined area has undergone Alpine metamorphism at lower greenschist facies conditions of about 450–550 °C and pressures between 3 and 5 kbar during Tertiary (FREY et al., 1980). Alpine chloritoid growth in metapelites is typical for these metamorphic conditions.

Most of the mineralized fissures are concentrated on one outcrop of unaltered dolomite in the riverbed of Val Renastga. Moreover some topaz-rich and hydrothermally altered sulfide-bearing dolomitic boulders with small crystals of goyazite were discovered downstream.

In the competent rock layers with boudinage structures (quartzites, dolomites) a lot of opened fissures and completely with quartz and carbonate filled veins are present. They can be divided into two groups:

- veins completely filled with quartz, carbonates and sulfide minerals (always without topaz), which strike east-west and dip steeply to south, often deformed in the main schistosity S_2 (ZK_a)
- fissures containing crystals of quartz, topaz and several other species which strike northwest-southeast and dip steeply to southwest (ZK_b); sometimes with fibrous quartz growth moretheless perpendicular to the wall-rock (RAMSAY, 1980). They are considered as tension fractures perpenticular to the stretching lineation l_2. They are a few centimeters long and less than 2 cm wide.

ZK_a veins are always crosscut by ZK_b fissures and are therefore older.

It is suggested that the formation of ZK_a predated that of S_2 while the later topaz-bearing clefts ZK_b were opened syn/post-S_2. Quartz in the older fissures has recrystallised textures without any measurable fluid inclusions. Fluid inclusions in ZK_b quartz allow to reconstruct the fluid evolution related to that later stage.

3. Fissure Paragenesis

The earlier veins (ZK_a) in the Triassic dolomite contain the following minerals: quartz, dolomite, pyrite, sphalerite, bournonite, tetrahedrite and galena (sulfide < 5 vol%). Pyrite occurs as idiomorphic grains < 20 μm together with sphalerite near the rim of the veins, as inclusions in galena and bournonite and disseminated in the dolomitic rocks. Larger pyrite grains show cataclastic features. Sphalerite also can be found intergrown with bournonite and tetrahedrite. Most of the ore minerals consist of

up to 1,5 mm large aggregates of bournonite and galena whereby bournonite is partly or completely replaced by galena.

In the opened fissures (ZK_b) the observed minerals (identified by a Bradley camera and FeK_α-radiation) are listed below:

- in Triassic dolomites topaz, quartz, dickite $Al_4[(OH)_8|Si_4O_{10}]$, (?) rutile, barite, apatite, goyazite $SrAl_3(PO_4)_2(OH)_5H_2O$, galena, sphalerite, tetrahedrite and secondary minerals (azurite, malachite and porous crusts of aragonite)
- in Triassic quartzites quartz and Fe-carbonates (altered)
- in Liassic limestones quartz, chlorite, muscovite, barite and calcite.

The quartz crystals have a maximal length of 2 cm and show besides the usual forms (m), (r) and (z) also accessory s-faces. They reveal few, but distinct sutures. Included in quartz are topaz, rutile, dickite, dolomite and bournonite/galena.

White, powder-like material which fills the bottom of the fissures was determined as dickite; this mineral is a polymorph variety of the more frequent alumosilicate kaolinite. At this locality topaz is always associated with dickite (plates ca 20 μm in diameter).

Of special interest are small, up to 1 mm long and brown-orange, pseudocubic crystals of goyazite which occur on sulfide- and topaz-bearing boulders.

White, milky and tabular aggregates, not longer than 2 cm, were recognized as barite. Galena forms irregular, corroded aggregates or short prismatic, distorted crystals. Tetrahedrite occurs as crystals up to 1 cm long and often with overgrowths of malachite.

Mineral succession in the topaz-bearing fissures is recorded as protogenetic inclusions in fissure quartz (Fig. 2). From geometric criteria the following succession of mineral phases is postulated:

- prismatic bournonite is formed during early quartz crystallization and later replaced by galena or completely dissolved forming longish pits at the basis of quartz
- early stage quartz includes rarely tiny, brownish needles (probably rutile)
- in late stage quartz topaz, dolomite and dickite are observed.

Dickite was deposited in one or several layers along the faces of growing quartz crystals. It is interesting to note that topaz was formed

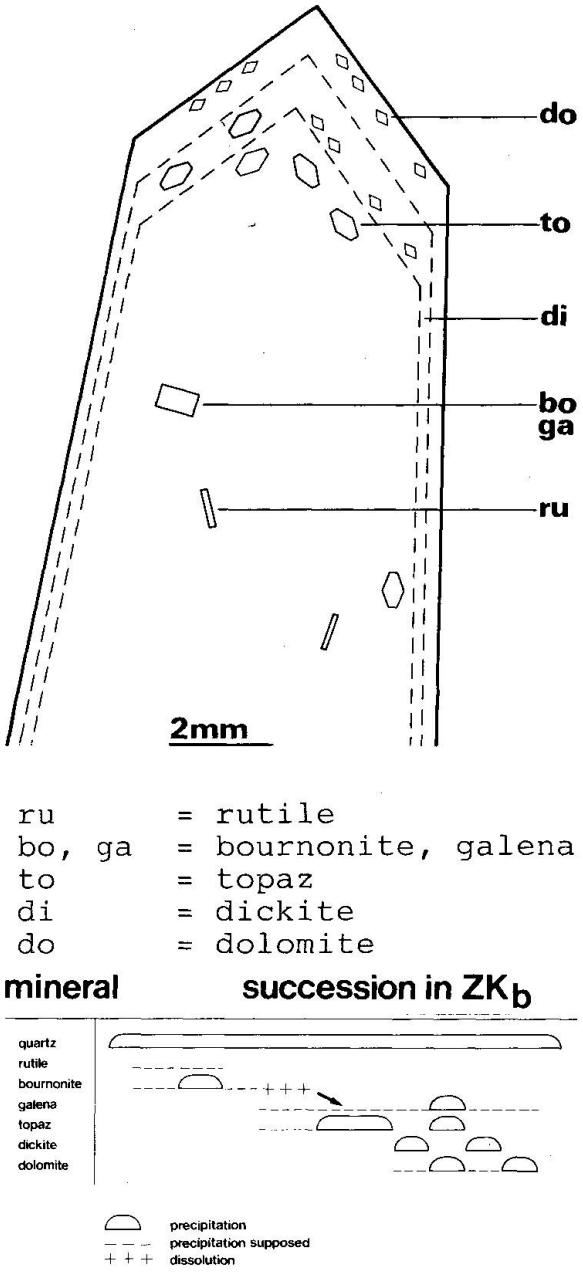

Fig. 2 Solid inclusions in fissure quartz and possible mineral succession.

preferentially before dickite or between several dickite layers, but never coexisted with dickite. Dolomite formation may be related to CO_2-rich fluid inclusions with variable gas content (type 4 a-b) and sulfide minerals (probably galena, tetrahedrite).

4. Description of Topaz

4.1. GENERAL CHARACTERIZATION

Topaz forms transparent yellowish to brown-orange, prismatic, needle-like crystals with a maximal length of 1.5 cm (Fig. 3). Ty-

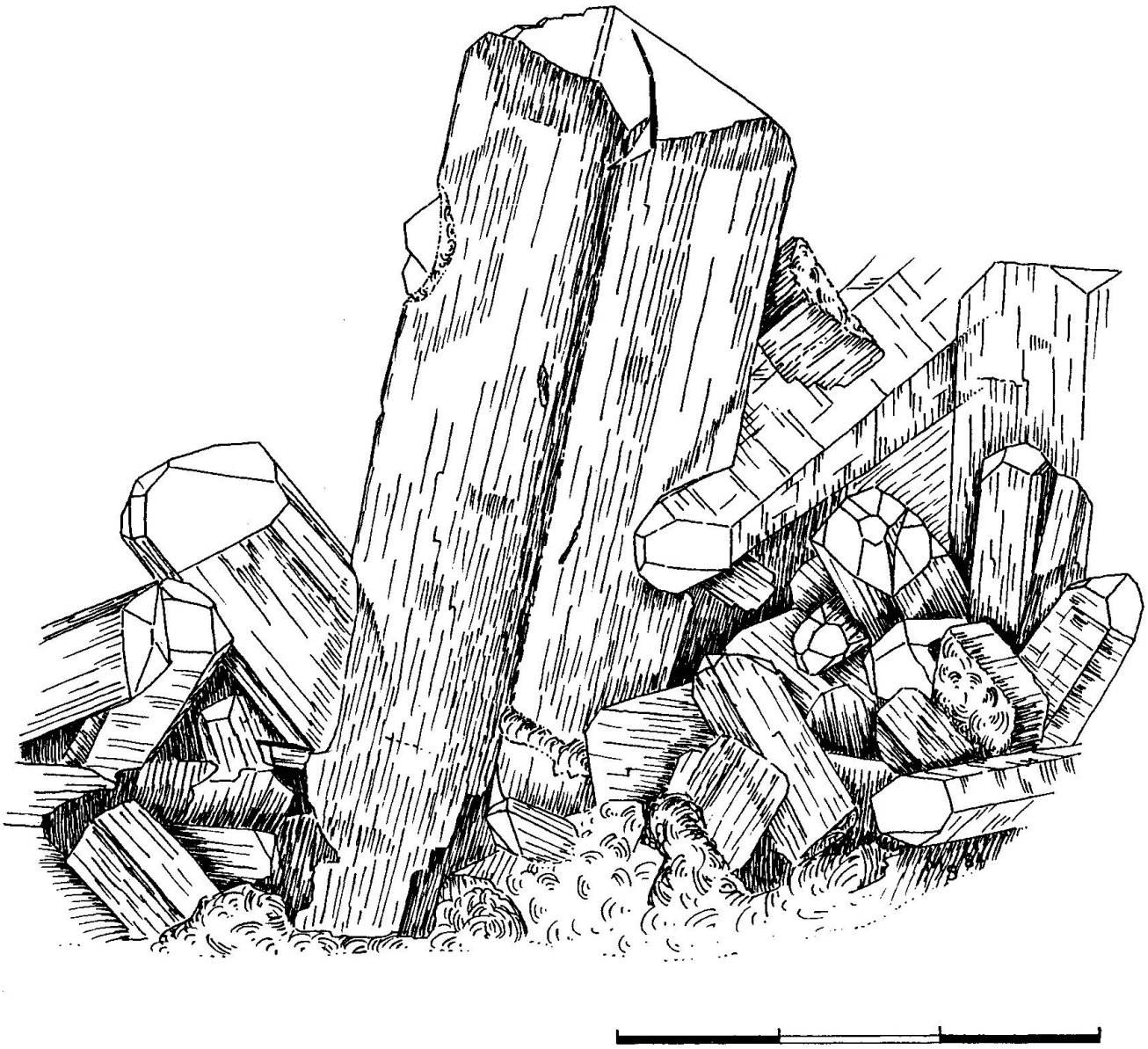

Fig. 3 Topaz and quartz specimen from Lugnez, scale mark = 3 mm.

pical forms are the prisms m (110), l(120), f (011) and dipyramides u (112). The pyramidal terminations display characteristically orthorhombic etch figures. Deep etch pits on the prisms are by far less frequent (Fig. 4).

On a single quartz specimen of 4.5 × 3 cm more than 100 topaz crystals between 1 and 10 mm length were observed. Most of them are intergrown with quartz and carbonates or cover the dolomite wallrock. Topaz has inclusions of dolomite and galena pseudomorph after bournonite.

In topaz thin sections viewed in (001) sectoral textures are recognized, which are typical for optically "anomalous" topaz (RINNE, 1926). According to AKIZUKI et al. (1979) and NEDER and BUSEK (1986) these sectors are differentiated primarily on the base of (F, OH) ordering and reveal varying optic axial angles. However, X-ray and optical determinative curves for OH/F in topaz cannot be applied on such ordered crystals (AKIZUKI et al., 1979).

4.2. EXPERIMENTAL

Several topaz crystals were heated for four hours at 950 °C to disorder OH/F and in turn to obtain material with uniform optical behavior (RINNE, 1926). Thermogravimetric experiments of HAMPAR and ZUSSMAN (1984) on topaz with a similar chemical composition (their T 20) indicated no significant weight loss below 1000 °C.

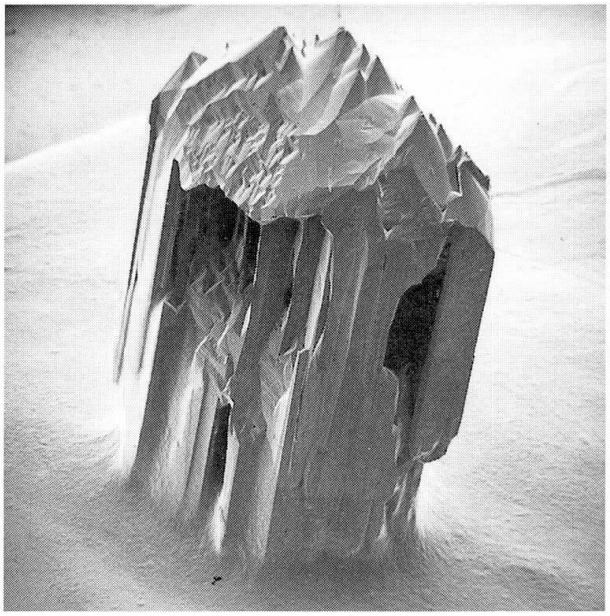

Fig. 4 Lugnez topaz with etch pits on prisms and dipyramid; size of crystal 1.5 mm. Photo by F. Zweili, Berne (No 2414/12).

For optical investigation and cell dimension measurements by X-rays one single heated topaz crystal (about 300 µm in diameter) was used.

4.3. OPTICAL PROPERTIES AND CELL DIMENSIONS

The topaz crystal was mounted on a glass fiber and positioned on a goniometer head. Subsequently, an extinction data set under crossed polarizers was collected on a spindle stage equiped microscope at 589.3 nm. The optic axial angle was refined with the program EXCALIBR (BLOSS, 1981) to $2V_z$:53 (1)°. The relatively low accuracy of the optic angle is mainly attributable to the high concentration of inclusions. Optic axial angles were also measured for selected domains of unheated topaz yielding $2V_z$ values of 42 (2)° and 47 (3)° respectively. Nevertheless these axial angles collected on zoned crystals are not representative (e.g. AKIZUKI et al., 1979).

Refractive indices (25 °C, 589.3 nm) along the principal vibration directions X and Z were estimated by the Becke method with appropriate immersion oils yielding $\alpha = 1.624$ (2) and $\gamma = 1.637$ (2). The same heated crystal was transferred to a CAD 4 (Enraf Nonius) 4-circle single-crystal diffractometer with graphite filtered MoKα-radiation. Single crystal X-ray reflections were sharp and no additional phases could be detected, which would indicate thermal decomposition of topaz (HAMPAR and ZUSSMAN, 1984). Cell dimensions were refined from the scattering vectors of 25 reflections between 5 and 25 °Θ.

4.4. F-OH SUBSTITUTION IN LUGNEZ TOPAZ

RIBBE and ROSENBERG (1971) use the optic angle $2V_z$, refractive indices, b cell dimension and unit cell volume to calculate the F-concentration in topaz.

This procedure was also applied to the investigated Lugnez sample leading to fluorine concentrations between 16 and 18 wt% (Tab. 1).

Tab. 1 F-concentration in Lugnez topaz estimated from optical properties and cell dimensions according to RIBBE and ROSENBERG (1971).

			F wt %
2 V z (°)	:	53	16.6
α	:	1.624	18.2
γ	:	1.637	16.2
b (Å)	:	8.820	17.6
V (Å)	:	344.04	18.2

However, if the regression line of KONNO and AKIZUKI (1982) is used the resulting F concentration (calculated from $2V_z$) is 15.7 wt% with a molar F/(F+OH) = 0.757. A possible maximal F-content of topaz is 20.7 wt%. All results indicate that the Lugnez topaz is relatively OH-rich. The highest so far recorded OH-content corresponds to approximately 30% replacement of F by OH (DEER et al., 1982).

5. Fluid Inclusions

Topaz crystallization took place during a relatively early stage of fissure-quartz growth. Thus early inclusions in quartz crystals also give information about the fluid phase during topaz formation. The size of the investigated inclusions varies from 10 µm to more than 500 µm. At room temperature in most of the inclusions three phases can be observed: an aqueous solution with a bubble of liquid and gase-

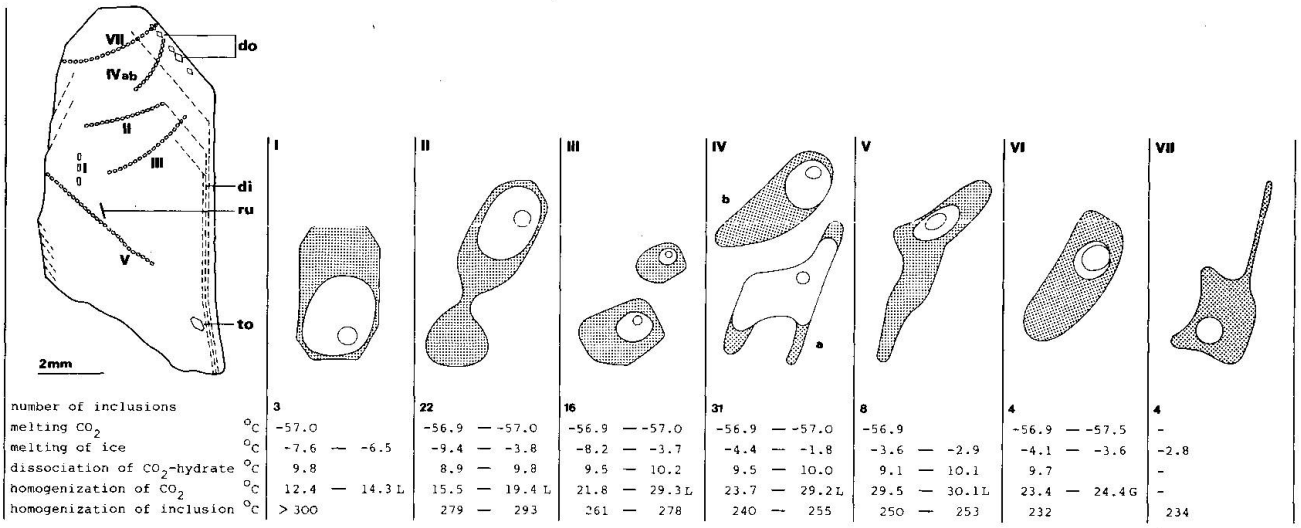

Fig. 5 Fluid evolution during quartz growth, Lugnez. Dolomite do, dickite di, rutile ru and topaz to.

ous CO_2. Dolomite, topaz and red-brownish needles - presumably rutile - were recognized as syngenetic solid inclusions characterising old growth surfaces. Tiny, isometric and colorless crystals occur in several inclusions and are stable at temperatures up to 300 °C. Nevertheless it seems they are real daughter minerals (probably carbonates).

5.1. EXPERIMENTAL

About 90 fluid inclusions were measured on four fissure quartz samples from Lugnez using a Leitz-microscope with a Chaix-Meca cooling and heating stage (POTY et al., 1976). Measured temperatures were corrected for systematic errors by measuring melting points of standard substances. Between -50° and +40 °C the accuracy of the measurement is within 0.1 °C, it is around 1° in the range 40-600 °C. The filling degree i.e. volume % of the liquid phase (vol) is estimated on the basis of graphical charts by ROEDDER (1984) and WALTHER (1981); accuracy is considered as ±10% of the estimated volume.

Tab. 2 Types of fluid inclusions in fissure quartz, Lugnez.

Type	ThCO2 (°C)		Th (°C)	
1	< 15	l	> 300	l
2	15-20	l	280-300	l
3	20-30	l	260-280	l
4a	20-30	l	245-255	g
4b	20-30	l	245-255	l
5	20-30	g	≈250	l
6	20-30	g	230-240	l
7	no CO_2 visible		≈230	l

5.2. RESULTS

According to the temperature of homogenization (Th) and the densities of CO_2, represented by the homogenization temperature of liquid and gaseous CO_2, the examined fluid inclusions are classified into seven different types (Tab. 2 + Fig. 5). The position of the planes with fluid inclusions within different quartz samples allows to correlate the planes with the precipitation of other mineral phases (for example dolomite, dickite) and to put them into a chronologic order. Inclusions of type 1 are presumably orientated along old growth surfaces and supposed to be primary, all the others are pseudosecondary. The relative succession of type 4 ab and 5 cannot be determined definitely in the examined quartz samples. Results are presented in Tab. 3.

The CO_2-bubbles decrease systematically from type 1 to type 7 from 35-40 to around 8 vol%. Only inclusions of type 4 ab have variable quantities of CO_2 from 20 to > 80 vol%, similar CO_2-densities and often occur within one fluid inclusion plane. They homogenize in the CO_2-rich (4a) or water-rich (4b) phase (Fig. 6 + 7a). Inclusions of this type are observed in late quartz and topaz precipitation. The coexis-

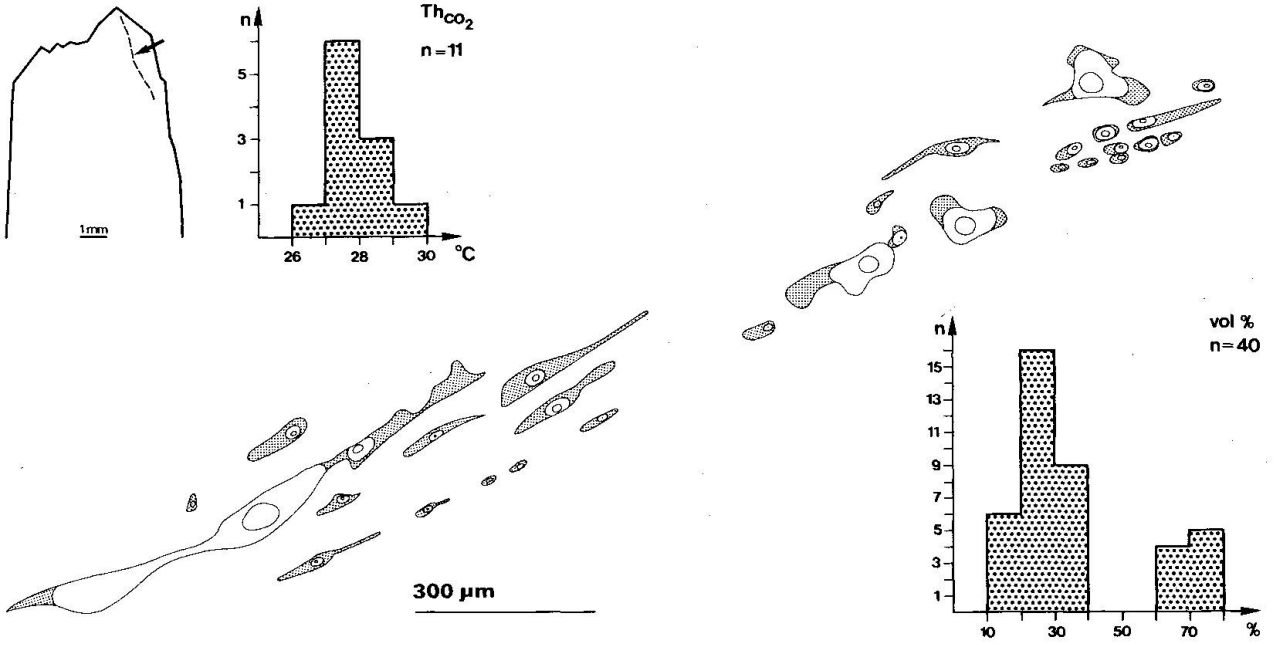

Fig. 6 Late inclusions in fissure quartz (type 4ab) with 20 to > 80 vol% CO_2 (vol) and homogenization of liquid and gaseous CO_2 into the liquid phase between 26.9 and 28.9 °C (T_{hCO_2}).

tence of inclusions with variable filling degree could be the effect of immiscibility at fluid trapping. On the contrary, necking down has been observed in 1-2% of all inclusions of every fluid type.

5.2.1. Salinity

The depression of the melting temperature of ice is a widely used methode to estimate salinity in fluid inclusions (ROEDDER, 1962). In the fluid inclusions from both quartz occurences in Lugnez, the first melting temperature (T_{m1}) is rather constant between -25 and -22 °C. This indicates that the dissolved salt components are dominated by NaCl and only minor amounts of other chlorides are present (ROEDDER, 1984).

The melting temperature (T_m) of quartz inclusions in the Triassic dolomites lies between -9.4 and -1.8 °C, in the quarzite it is around -2.7 °C (Fig. 7b). Early fluid types show generally lower melting temperatures than late ones. In the system H_2O-CO_2-NaCl these values cannot be used for direct estimation of the salinity of the aqueous solution: the main reason for this is, that in the inclusions no equilibrium-conditions can be measured. Experiments show that T_m can be varied by the speed of cooling. During this process H_2O will be incorporated in the CO_2-clathrate, which raises the salt content of the residual solution (COLLINS, 1979). Repeated cooling and heating below 0 °C (this means without dissociation of CO_2-clathrate) of a single inclusion (type 3) from Lugnez showed a gradual enrichment in the salt content of the residual solution. The value of T_m decreased from -3.8 to -21 °C which corresponds to the eutectical temperature in the system H_2O-NaCl (Fig. 7c). With each cooling step H_2O was removed from the solution and incorporated in more and more CO_2-clathrate.

It is worth noting that in the salt-free system H_2O-CO_2, the melting point of ice in presence of a liquid CO_2-phase is not 0% but -1.48 °C (BOZZO et al., 1973).

The measurements of T_{m1} and T_m point up to three facts: the aqueous solutions have a certain salt content, the salt is mainly NaCl and the salt content seems to decrease from type 1 to type 7. In the pure, saltfree system H_2O-CO_2 the CO_2-clathrate dissociates at 10 °C and 45 bars (WIEBE and GADDY, 1940; TAKENOUCHI and KENNEDY, 1965). The addition of salt components lowers this temperature (T_d). This fact can be used to determine the real salt content in a fluid inclusion. In the quartz crystals from Lugnez the T_d is between +8.9 and +10.2 °C (Fig. 7d). Calculated salinities according to COLLINS (1979) and BOZZO et al. (1973) are in a

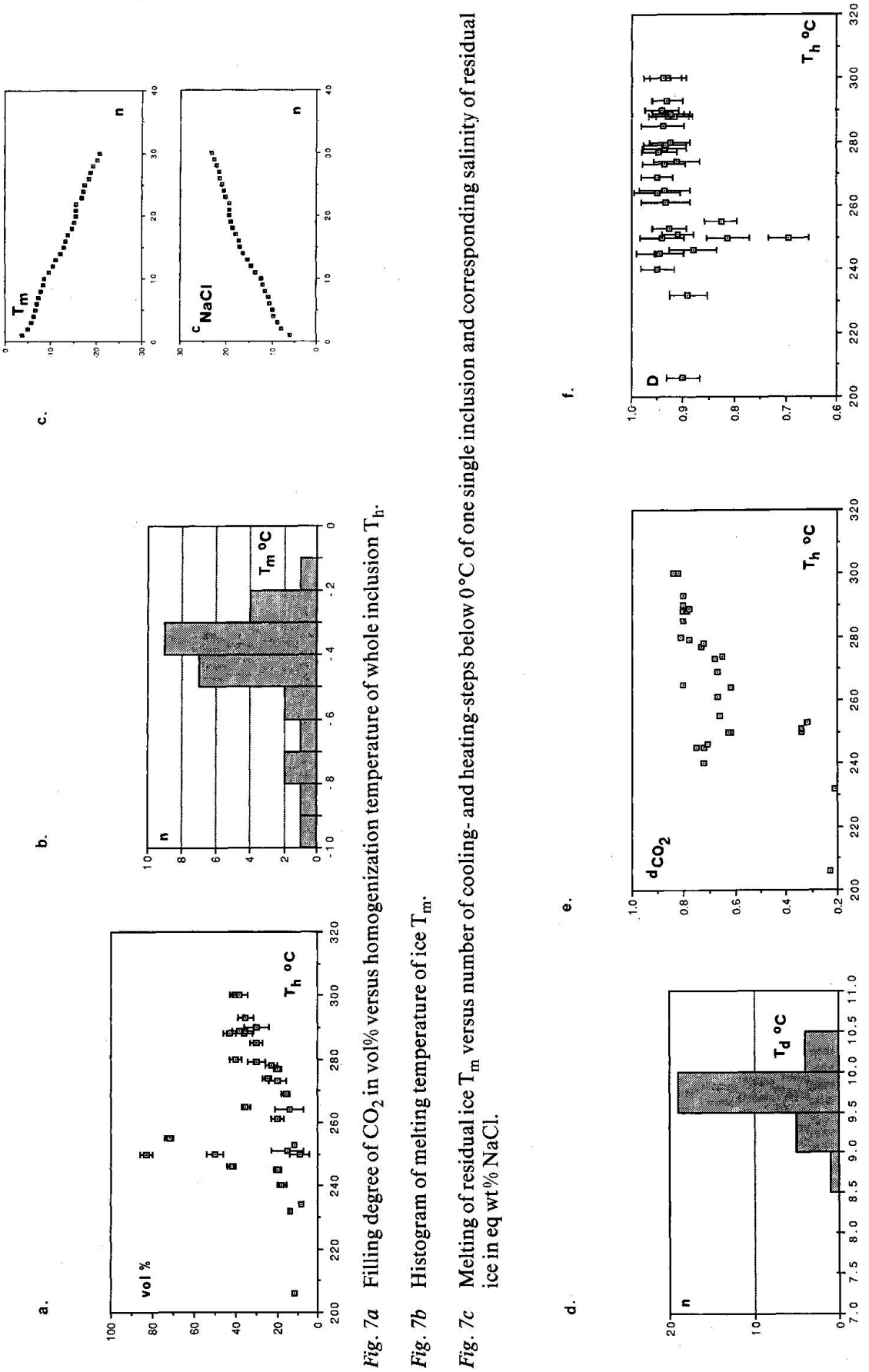

Fig. 7a Filling degree of CO_2 in vol% versus homogenization temperature of whole inclusion T_h.

Fig. 7b Histogram of melting temperature of ice T_m.

Fig. 7c Melting of residual ice T_m versus number of cooling- and heating-steps below 0 °C of one single inclusion and corresponding salinity of residual ice in eq wt% NaCl.

Fig. 7d Histogram of dissociation temperature of CO_2-clathrate T_d.

Fig. 7e Density of CO_2-rich part d_{CO_2} versus T_h.

Fig. 7f Density of homogenized inclusion D versus T_h.

relatively narrow range between 2.2 and 0.4 equivalent weight % NaCl (mean of different fluid types). They show no systematic trend during fluid evolution and are in contrast to the described values derived from the measurements of T_m. In about 10% of the measured inclusions T_d is > 10.0°C. It seems that the system H_2O-CO_2-NaCl is not pure. In fact gas species like CH_4, H_2S, N_2,... shift T_d to values above 10°C. On crushing the quartz crystals one can smell a moderate but typical H_2S odour. Only measurements by Raman spectroscopy could give quantitative values for the gas species which are microthermometrically not detectable.

For further estimations, salinities are calculated on the base of dissociation temperature of CO_2-clathrate. They are considered as minimal values for real salt content.

5.2.2. Carbon dioxide

CO_2 can be detected in nearly all inclusions. The triple point of CO_2 is situated at -56.6°C and decreases when other gases are added (UNRUH and KATZ, 1949; HOLLISTER and BURRUS, 1976). Measured values of CO_2 melting range between -56.9 and -57.5°C. Values below -57.0°C have been observed in late fluid type 6. The existence of minor amounts of H_2S in the fluid (see above) is also supported by the occurence of several sulfide minerals in the topaz bearing fissures.

The homogenization of the non-aqueous part is for the inclusion of type 1 to 4 in the liquid phase; the T_{hCO_2} lies between 12.4 and 29.2°C corresponding to a density from 0.84 to 0.62 g/cm³ for pure CO_2. The inclusions of type 5 and 6 homogenize in the vapour phase; the T_{hCO2} is between 30.1 and 23.4°C, what corresponds to a density of 0.34 to 0.21 g/cm³ for pure CO_2 (WEAST, 1980, Fig. 7e).

5.2.3. Density and estimated composition

The density of the whole inclusion is calculated from the filling degree and the densities of water and CO_2 (TOURET, 1977). The density of water depends primarily on the salinity and can be estimated by aid of the data in POTTER and BROWN (1977). The density of the whole inclusion decreases slightly during fluid evolution from 0.97 to 0.91 g/cm³ with an abrupt descent in fluid type 4a down to 0.70 g/cm³ due to high CO_2-content (Fig. 7f).

The approximate composition of inclusions can be calculated from the filling degree and the density of CO_2, water and the salinity, and is given in mol% (see MULLIS, 1987). The concentrations of CO_2 vary between 56 and 3 mol%, those of NaCl (eq) between 2.2 and 0.1 mol%. Mainly due to the unprecise estimation of the filling degree, relative errors on such calculations are considerably high i.e. around 30%.

5.2.4. Homogenization temperature and isochores

Except for fluids of type 4a all the other ones homogenized in the liquid, water-rich phase. Most of the inclusions of type 4a decrepitate before homogenization, but those of smaller size show a homogenization in the CO_2-rich vapour phase. This is considered as a further criterion for CO_2-water unmixing towards the end of mineralization.

Homogenization temperature of the whole fluid inclusion can be considered as minimal formation temperature, provided that the inclusion was homogenous on trapping. The measured values are from 230 to > 300°C. To obtain the real forming temperature however a major pressure correction is necessary.

In a PT-diagram the isochores for some of the measured three-phase-inclusions have been constructed according to BOWERS and HELGESON (1983) for the pure H_2O-CO_2-NaCl system. In the diagram are also indicated the maximal PT-conditions of the Alpine metamorphism for the wider environments of Val Lugnez (area A in Fig. 8) according to FREY et al. (1980). Finally lithostatic and hydrostatic gradients for an average density of 2.6 resp. 1.0 g/cm³ have been calculated for different thermogradients. Minimal pressures for fluid type 1-3 are 2.9-3.2 kbar.

5.2.5. Discussion

The Lugnez topaz was formed in a low saline, preferentially NaCl-bearing, hydrothermal solution with relatively high amount of CO_2. The CO_2-content in early stage mineralization of > 10 mol% CO_2 is characteristic of mesometamorphic fluid compositions in the

Tab. 3a Measured temperatures in °C.

Dolomite

type	n	vol%	∂vol%	TmCO2	∂TmCO2	TmH2O	∂TmH2O	Td	∂Td	ThCO2	∂ThCO2			Th	∂Th		Sample
1	1	40	4	-57.0	0.1	-6.5	0.1	9.8	0.1	14.3	0.1	l	>	300	1	l	LU 11
1	2	38	4	-57.0	0.1	-7.6	0.1	9.8	0.1	12.4	0.4	l	>	300	1	l	LU 11
2	2	35	4	-57.0	0.1	-5.7	0.1	9.8	0.1	16.1	0.1	l		293	1	l	LU 11
2	2	30	3	-56.9	0.1	-3.8	0.1	9.7	0.1	17.2	0.1	l		290	2	l	LU 11
2	4	35	6	-56.9	0.1	-9.4	0.1	9.1	0.1	18.8	0.1	l		289	1	l	LU 1
2	2	38	4	-56.9	0.1			9.0	0.1	19.4	0.1	l		289	1	l	LU 1
2	2	36	4	-57.0	0.1	-5.0	0.1	9.8	0.1	16.8	0.1	l		288	1	l	LU 11
2	2	43	4	-56.9	0.1			8.9	0.1	18.3	0.1	l		288	1	l	LU 1
2	3	30	3	-56.9	0.1					16.6	0.1	l		285	2	l	LU 11
2	1	40	4	-57.0	0.1	-5.8	0.1	9.8	0.1	15.5	0.1	l	>	280	1	l	LU 11
2	3	30	3	-57.0	0.1	-4.5	0.1	9.8	0.1	18.7	0.1	l		279	4	l	LU 11
2	1	35	4	-56.9	0.1	-7.2	0.1	9.1	0.1	16.2	0.1	l	>	265	1	l	LU 1
3	2	23	3	-56.9	0.1			9.8	0.1	23.8	0.1	l		278	1	l	LU 11
3	5	20	4	-56.9	0.1	-4.8	0.1	9.7	0.1	23.6	0.1	l		277	2	l	LU 11
3	1	25	3	-57.0	0.1	-3.5	0.1	9.8	0.1	28.0	0.1	l		274	1	l	LU 11
3	1	20	2	-56.9	0.1	-4.3	0.5	9.8	0.1	26.7	0.1	l		273	1	l	LU 11
3	2	16	2	-56.9	0.1	-3.9	0.1	9.5	0.1	27.3	0.1	l		269	1	l	LU 1
3	2	14	2	-56.9	0.1	-8.2	0.3	9.5	0.2	29.3	0.1	l		264	1	l	LU 1
3	1	20	2	-56.9	0.1					27.2	0.1	l		261	1	l	LU 1
3	1	20	2	-56.9	0.1	-4.3	0.1			22.0	0.1	l	>	245	1	l	LU 1
3	1	30	3	-56.9	0.1	-3.7	0.1	10.2	0.1	21.8	0.1	l					LU 14
4a	8	72	7	-57.0	0.1	-2.4	0.2	10.0	0.1	27.7	0.2	l		255	2	g	LU 11
4a	1	50	5	-57.0	0.1	-1.8	0.1	9.5	0.1	29.2	0.1	l	>	250	1	g	LU 11
4a	2	83	8	-56.9	0.1	-2.3	0.1	10.0	0.1	28.7	0.2	l	>	250	1	g	LU 11
4a	10	68	7							27.2	0.3	l					LU 13
4a	3	42	3	-56.9	0.1	-3.3	0.1	9.6	0.1	24.6	1.1	l		246	1	l	LU 1
4b	5	20	4	-57.0	0.1	-4.4	0.1	9.8	0.1	24.2	0.1	l		245	1	l	LU 11
4b	2	18	2	-57.0	0.1	-4.0	0.1	9.8	0.1	23.7	0.1	l		240	3	l	LU 11
5	3	12	3	-56.9	0.1	-3.6	0.1	9.2	0.2	29.5	0.1	g		253	1	l	LU 1
5	1	15	2	-56.9	0.1	-3.5	0.1	9.1	0.1	30.1	0.1	g		251	1	l	LU 1
5	4	9	1	-56.9	0.1	-2.9	0.1	10.1	0.1	29.8	0.1	g		250	2	l	LU 11
6	3	14	2	-57.5	0.1	-3.6	0.1	9.7	0.1	23.4	0.4	g		232	1	l	LU 11
6	1	12	1	-56.9	0.1	-4.1	0.1			24.4	0.1	g	>	206	1	l	LU 1
7	4	8	2			-2.8	0.1	9.7	0.1					234	2	l	LU 11

Quartzite

type	n	vol%	∂vol%	TmCO2	∂TmCO2	TmH2O	∂TmH2O	Td	∂Td	ThCO2	∂ThCO2			Th	∂Th		Sample
1	9	10	2			-2.7	0.2							221	6	l	LU 7
2	1	8	1	-57.3	0.1	-2.1	0.1	10.2	0.1	25.1	0.1	g	>	177	1	l	LU 7

Measured Values:

type of inclusion according to Tab 2
n : number of inclusions
vol : estimated volume of CO_2-rich part
T_{mCO2} : Temperature of melting of CO_2
T_{mH2O} : Temperature of complete melting of H_2O
T_d : Temperature of dissociation of CO_2-clathrate
T_{hCO2} : Temperature of homogenization of CO_2 into liquid (l) and gas (g) phase
T_h : Temperature of homogenization of inclusion into liquid (l) and gas (g) phase

Tab. 3b Calculated values based on the measured temperatures. δ indicates always the uncertainty, i.e. ± δ in absolute values.

Dolomite

type	cNaCl*	∂cNaCl*	cNaCl**	∂cNaCl**	dH2O**	∂dH2O**	d CO2	∂dCO2	D	∂ D	CO2	∂CO2	NaCl	∂NaCl	
1	9.8	0.1	0.4	0.2	1.001	0.002	0.82	0.01	0.929	0.031	19.6	8.1	0.1	0.2	PT
1	11.2	0.1	0.4	0.2	1.001	0.002	0.84	0.01	0.940	0.032	18.8	8.2	0.1	0.2	
2	8.8	0.1	0.4	0.2	1.001	0.002	0.80	0.01	0.931	0.034	16.5	7.7	0.1	0.2	
2	6.1	0.1	0.6	0.2	1.002	0.002	0.80	0.01	0.941	0.036	13.9	5.9	0.2	0.3	
2	13.3	0.1	1.8	0.2	1.011	0.002	0.78	0.01	0.930	0.036	16.2	10.8	0.5	0.4	
2			2.0	0.2	1.013	0.002	0.78	0.01	0.924	0.036	17.8	7.7	0.5	0.3	
2	7.9	0.1	0.4	0.2	1.001	0.002	0.80	0.01	0.929	0.033	17.0	7.8	0.1	0.2	
2			2.2	0.2	1.014	0.007	0.79	0.01	0.918	0.030	20.9	8.1	0.6	0.3	
2							0.80	0.01	0.940	0.036	13.8	6.0			*
2	8.9	0.1	0.4	0.2	1.001	0.002	0.81	0.01	0.925	0.031	19.5	8.1	0.1	0.2	
2	7.2	0.1	0.4	0.2	1.001	0.002	0.78	0.01	0.935	0.036	13.6	5.8	0.1	0.3	PT
2	10.7	0.1	1.8	0.2	1.011	0.002	0.80	0.01	0.937	0.034	16.5	7.7	0.5	0.3	
3			0.4	0.2	1.001	0.002	0.72	0.01	0.936	0.039	9.8	5.2	0.1	0.3	
3	7.6	0.1	0.6	0.2	1.002	0.002	0.73	0.01	0.948	0.042	8.7	6.7	0.2	0.3	
3	5.7	0.1	0.4	0.2	1.001	0.002	0.65	0.01	0.913	0.039	9.9	4.9	0.1	0.3	
3	6.9	0.8	0.4	0.2	1.001	0.002	0.68	0.01	0.937	0.041	8.3	3.6	0.1	0.3	PT
3	6.3	0.1	1.0	0.2	1.005	0.002	0.67	0.01	0.951	0.043	6.8	3.5	0.3	0.3	
3	12.0	0.4	1.0	0.4	1.005	0.003	0.62	0.01	0.951	0.044	5.8	3.2	0.3	0.6	
3							0.67	0.01	0.934	0.041	8.2	3.6			*
3	6.9	0.1					0.75	0.01	0.950	0.040	8.9	3.1			*
3	6.0	0.1					0.75	0.01	0.925	0.036	13.2	5.7			*
4a	4.0	0.3					0.66	0.01	0.827	0.031	45.1	19.3			*
4a	3.1	0.1	1.0	0.2	1.005	0.002	0.62	0.01	0.813	0.032	21.5	8.7	0.3	0.2	PT
4a	3.9	0.1					0.63	0.01	0.693	0.031	56.1	25.6			*
4a							0.67	0.02	0.776	0.031	37.6	16.5			*
4a	5.4	0.1	0.8	0.2	1.004	0.002	0.71	0.01	0.881	0.031	18.8	5.9	0.2	0.2	
4b	7.0	0.1	0.4	0.2	1.001	0.002	0.72	0.01	0.945	0.042	8.6	8.1	0.1	0.3	
4b	6.4	0.1	0.4	0.2	1.001	0.002	0.72	0.01	0.950	0.041	7.9	3.7	0.1	0.3	
5	5.8	0.1	1.6	0.4	1.01	0.002	0.32	0.01	0.927	0.049	3.7	2.6	0.5	0.7	
5	5.7	0.1	1.8	0.2	1.011	0.002	0.34	0.01	0.910	0.045	4.3	2.1	0.6	0.3	PT
5	4.8	0.1					0.34	0.01	0.941	0.046	3.3	1.5			*
6	5.8	0.1	0.6	0.2	1.002	0.002	0.21	0.01	0.891	0.046	3.3	1.6	0.2	0.3	PT
6	6.6	0.1					0.23	0.01	0.901	0.045	3.2	1.4			*
7	4.6	0.1	0.6	0.2	1.002	0.002									PT

Quartzite

type	cNaCl*	∂cNaCl*	cNaCl**	∂cNaCl**	dH2O*	∂dH2O*	d CO2	∂dCO2	D	∂ D	CO2	∂CO2	NaCl	∂NaCl	
1	4.5	0.3			1.022	0.001			0.925	0.01			2.2	0.2	
2							0.23	0.01	0.938	0.02	3.0	1.2			*

Estimated Values:

cNaCl* : Salinity of residual solution according to COLLINS (1979) [eq wt % NaCl]

dH2O* : Density of aqueous solution with salinity cNaCl* [g/cm^3]

cNaCl** : Salinity of aqueous solution calculated on T_d according to BOZZO et al (1973) [eq wt % NaCl]

dH2O** : Density of aqueous solution with salinity cNaCl** [g/cm^3]

dCO2 : Density of homogenized CO_2 into the liquid (l) and gas (g) phase according to WEAST (1980) [g/cm^3]

D : Density of whole inclusion according to TOURET (1977) (g/cm3)

CO_2, NaCl : approximative composition of fluid inclusion for the pure system H_2O-CO_2-NaCl (mol%) and aqueous solution with 5 wt % CO_2 and salinity cNaCl** according to MULLIS (1987). PT: data used for isochore constructions

Alps (FREY et al., 1980). In Lugnez such CO_2-rich fluids are recorded in fissure quartz within epimetamorphic dolomites a few hundred meters below the thrust zone of the Pennine nappes. A mesometamorphic origin for these fluids is supported by the isochores in Fig. 8 which seem to reflect higher metamorphic conditions than those estimated for Lugnez. The formation of CO_2 in fluids from Alpine fissure quartz is discussed in HOEFS and STALDER (1977) and is mainly caused by decarbonation reactions, dissolution of carbonates; or is perhaps of juvenile origin.

The fluid evolution recorded in the examined quartz samples shows a retrograde behaviour with decreasing CO_2-content. The crystallization of topaz and dickite was probably directed by slight shifts in pH and changes in F-fugacities.

Towards the end of mineralization occurred at around 250 °C-water unmixing. There was liberated a CO_2-rich phase, which was included in various gas-liquid proportions in late stage quartz and topaz. Simultaneously, dolomite and sulfide minerals were precipitated. The sudden diminution in fluid density could be caused by abrupt diminution in pressure from lithostatic to hydrostatic conditions at thermogradients of 25 ± 5 °C/km. Sudden decrease in pressure and subsequent gas-water unmixing in Alpine fissures was first recognized by MULLIS (1976) in CH_4-bearing skeletal quartz from Val d'Illiez and explained with abrupt opening and fissure enlargement through tectonic activity. Skelettal quartz with variable amounts of different gas species as CH_4, CO_2, N_2 etc. due to pressure drops and CO_2-water unmixing is supposed to be widespread in the Alps (MULLIS, 1983). Unmixing of the fluid phase during Alpine metamorphism was also described by MERCOLLI (1982) and TROMMSDORFF and SKIPPEN (1986) from Campolungo area.

The PT interval between maximal conditions of Alpine metamorphism of 500–550 °C and 3-5 kbar and the unmixing of the fluid phase around 250 °C and 1 kbar (hydrostatic pressure) can be considered as estimation for the conditions of topaz growth in Lugnez.

6. Other topaz occurrences

Topaz occurs essentially in acid igneous rocks and in high or low stage hydrothermal deposits. The F-content in natural topaz varies between 20.4 and 13.4 wt% (DEER et al., 1982). The replacement of F by OH depends on pressure, temperature and fugacities of HF and H_2O (ROSENBERG, 1972).

The Lugnez topaz has been found as a hydrothermal mineral in an Alpine fissure, crystallized at the end of the Alpine orogeny. The topaz is relatively OH-rich with a molar value of F/(F+OH) = 0.757, calculated from $2V_z$ after heat-treatment. In the following, the Lugnez topaz should be compared with similar topaz crystallizations.

The alpine topaz studied by ZEMANN et al. (1979) from pegmatoid quartz-dikes in Untersulzbachtal was optically homogenious even without heat treatment a = 4.6651 (11) Å, b = 8.8381 (39) Å, c = 8.3984 (65) Å. A microprobe analysis indicated F/(F+OH) = 0.72 which is in agreement with the b-axis dimension according to RIBBE and ROSENBERG (1971) leading to 15.8 wt% F. Topaz from Ouro Preto / Brasil described in THOMAS (1982) shows similar F-content of 16.0 wt% and homogenization temperatures of fluid inclusions about 270 ± 11 °C. The experimental data of ROSENBERG (1972) indicate that OH-rich/F-poor topaz forms preferentially in low temperature conditions. This is also confirmed by the fluid inclusion measurements on coexisting quartz.

Another similarity between the Austrian topaz and our sample is the assemblage with dickite (MEIXNER, 1978). In the Swiss Alps dickite has been described from ankerite-rich fissures in the Gotthard-Tunnel (GRAESER and STALDER, 1974; STALDER et al., 1980). Dickite is reported from Kansas as void-filling mineral in limestones intruded by igneous rocks (HAYES, 1967) and as cement and vein-filling silicate in epigenetic sandstones (SHUTOV et al., 1970). KANTOROWICZ (1984) describes dickite as authigenic clay mineral in jurassic sandstones and relates dickite formation to the reaction of CO_2-bearing, acidic fluids with carbonate cemented rocks. In Lugnez similar reactions are probable and the CO_2-bearing fluid is documented in inclusions from fissure quartz.

Acknowledgment

We are indebted to H. Luginbühl, Windisch, who provided excellent samples for investigation. Many helpful advices and communications we received from Mrs. Dr. Cl. Ramboz, Nancy. She also calcu-

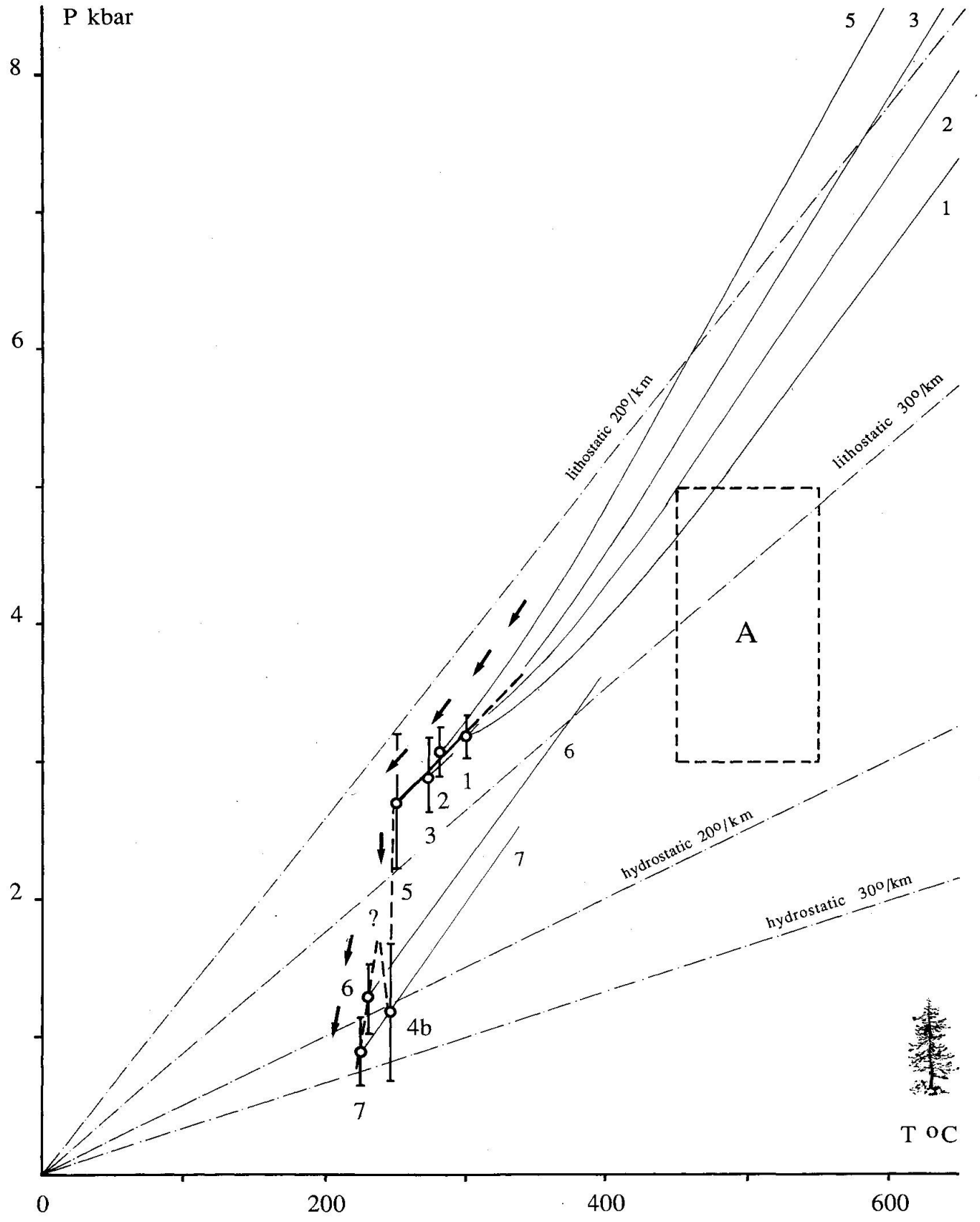

Fig. 8 Isochores in pT-diagram for different fluid types 1–7 according to BOWERS and HELGESON (1983). Field A: maximal pT-conditions for Alpine metamorphism in Lugnez according to FREY et al. (1980).

lated the plotted isochores from Fig. 8. Her help is greatly appreciated. We also thank Dr. J. Mullis, Basel, for constructive suggestions for improvement of the manuscript and Prof. W.K. Nabholz for discussions about the regional geology. B. Hurfurd, London, and Dr. J.J. Oberling corrected the English of this paper.

References

AKIZUKI, M., HAMPAR, M.S. and ZUSSMANN, J. (1979): An explanation of anomalous optical properties of topaz. Min. Mag. 43, 237–241.

BLOSS, F.D. (1981): The spindle stage: principles and practice. Cambridge University Press.

BOWERS, T.S. and HELGESON, H.C. (1983): Calculation of the thermodynamic and geochemical consequences of nonideal mixing in the system H_2O-CO_2-NaCl on phase relations in geologic systems: Equation of state for H_2O-CO_2-NaCl fluids at high pressures and temperatures. Geochim. Cosmochim. Acta 47, 1247–1275.

BOZZO, A.T., CHEN, H.S., KASS, J. and BARDUHN, A.J. (1973): The properties of the hydrates of chlorine and carbon dioxide. Int. Symp. Fresh Water from the Sea 3, 437–451.

COLLINS, P.L.F. (1979): Gas hydrates in CO_2-bearing fluid inclusions and the use of freezing data for estimation of salinity. Econ. Geol. 74, 1435–1444.

DEER, W.A., HOWIE, R.A. and ZUSSMAN, J. (1982): Rock-forming Minerals. Vol. 1A Orthosilicates. Longman, Second Edition, London and New York.

FREY, M., BUCHER, K., FRANK, E. and MULLIS, J. (1980): Alpine metamorphism along the Geotraverse Basel-Chiasso – a review. Eclogae geol. Helv. 73/2, 527–546.

GRAESER, S. and STALDER, H.A. (1974): Mineral-Neufunde aus der Schweiz und angrenzenden Gebieten. Schweizer Strahler 3, 265–277.

HAMPAR, M.S. and ZUSSMANN, J. (1984): The thermal breakdown of topaz. Tschermaks Min. Petr. Mitt. 33, 235–252.

HAYES, J.B. (1967): Dickite in Lansing group (Pennsylvanian) limestones, Wilson and Montgomery Counties, Kansas. Amer. Mineralogist 52, 890–896.

HOEFS, J. and STALDER, H.A. (1977): Die C-Isotopenzusammensetzung von CO_2-haltigen Flüssigkeitseinschlüssen in Kluftquarzen der Zentralalpen. Schweiz. mineral. petrogr. Mitt. 57, 329–347.

HOLLISTER, L.S. and BURRUSS, R.C. (1976): Phase equilibria in fluid inclusions from the Khtada Lake metamorphic complex. Geochim. Cosmochim. Acta 40, 163–175.

JUNG, W. (1963): Die mesozoischen Sedimente am Südostrand des Gotthard-Massivs (zwischen Plaun la Greina und Versam). Eclogae geol. Helv. 56/2, 653–754.

KANTOROWICZ, J. (1984): The nature, origin and distribution of authigenic clay minerals from middle Jurassic Ravenscar and Brent Group sandstones. Clay Miner. 19, 359–375.

KONNO, H. and AKIZUKI, M. (1982): Fluorine determination and relation between fluorine content and 2V value of topaz. N.Jb. Mineral. Mh. 10, 465–470.

MEIXNER, H. (1961): Das Vorkommen schöner Topas-Kristalle in den Hohen Tauern Salzburgs. Fortschr. Mineral. 39/1, 82–83.

MEIXNER, H. (1978): Topas-Kristalle von der Stokkeralm im Untersulzbachtal, Salzburg. Lapis (3) 7/8, 58–59.

MERCOLLI, I. (1982): Le inclusioni fluide nei noduli di quarzo di marmi dolomitici della regione del Campolungo (Ticino). Schweiz. mineral. petrogr. Mitt. 62, 245–312.

MULLIS, J. (1976): Das Wachstumsmilieu der Quarzkristalle im Val d'Illiez (Wallis, Schweiz). Schweiz. mineral. petrogr. Mitt. 56, 219–268.

MULLIS, J. (1983): Einschlüsse in Quarzkristallen der Schweizer Alpen und ihre mineralogisch-geologische Bedeutung. Bull. Soc. Frib. Sc. Nat. 72, 5–19.

MULLIS, J. (1987): Fluid inclusion studies during very low-grade metamorphism. – In: FREY, M. (1987): Low temperature metamorphism. Blackie, Glasgow, 162–199.

NABHOLZ, W.K. and VOLL, G. (1963): Bau und Bewegung im gotthardmassivischen Mesozoikum bei Ilanz (Graubünden). Eclogae geol. Helv. 56/2, 755–808.

NEDER, R. and BUSEK, P.R. (1986): Sensitivity of convergent-beam electron diffraction to F-OH order-disorder in topaz. Zeitschr. Kristallogr. 174, 156–157.

POTTER, R.W. and BROWN, D. (1977): The volumetric properties of aqueous sodium chloride solutions for 0° to 500 °C at pressures up to 2000 bars based on a regression of available data in the literature. U.S. geol. Survey Bull. 1421-C.

POTY, B.P., LEROY, J. and JACHIMOWICZ, L. (1976): Un nouvel appareil pour la mesure des températures sous le microscope: l'installation microthermométrie Chaixmeca. Bull. Soc. fr. Minéral. Cristallogr. 99, 182–186.

RAMSAY, J.G. (1980): The crack-seal mechanism of rock deformation. Nature 284, 135–139.

RIBBE, P.H. (1982): Topaz. In: RIBBE, P.H. (Ed): Orthosilicates. Reviews in mineralogy 5, 215–230.

RIBBE, P.H. and ROSENBERG, P.E. (1971): Optical and X-ray determinative methods for fluorine in topaz. Amer. Mineralogist 56, 1812–1821.

RINNE, F. (1926): Bemerkungen über optische Anomalien, insbesondere des brasilianer Topas. Z. Kristallogr. 63, 236–246.

ROEDDER, E. (1962): Studies of fluid inclusions I: Low temperature application of a dual-purpose freezing and heating stage. Econ. Geol. 57, 1045–1061.

ROEDDER, E. (1984): Fluid Inclusions. Reviews in Mineralogy 12.

ROSENBERG, P.E. (1972): Compositional variations in synthetic topaz. Amer. Mineralogist 57, 169–187.

SHUTOV, V.D., ALEKSANDROVA, A.V. and LOSIEVSKAYA, S.A. (1970): Genetic interpretation of the polymorphism of the kaolinite group in sedimentary rocks. Sedimentology 15, 69–82.

STALDER, H.A., SICHER, V. and LUSSMANN, L. (1980): Die Mineralien des Gotthardbahntunnels und des Gotthardstrassentunnels N2. Repof AG, Gurtnellen.

TAKENOUCHI, S. and KENNEDY, G.C. (1964): The binary system H_2O-CO_2 at high temperatures and pressures. Amer. J. Sci. 263, 445–454.

THOMAS, R. (1982): Ergebnisse der thermobarogeochemischen Untersuchungen an Flüssigkeitseinschlüssen in Mineralien der postmagmatischen Zinn-Wolfram-Mineralisation des Erzgebirges. Freiberger Forschungsh. C 370.

TOURET, J. (1977): The significance of fluid inclusions in metamorphic rocks. In D.G. FRASER, ed., Thermodynamics in Geology. D. Reidel Publ. Co., Dordrecht, The Netherlands, 203–227.

TROMMSDORFF, V. and SKIPPEN, G. (1986): Vapour loss ("boiling") as a mechanism for fluid evolution in metamorphic rocks. Contrib. Mineral. Petrol. 94, 317–322.

TRUNINGER, E. (1911a): Geologisch-petrographische Studien am Gasternmassiv. Mitt. natf. Ges. Bern 1911.

TRUNINGER, E. (1911b): Kontaktmetamorphe Erscheinungen im westlichen Teil des Aarmassivs (Gasternmassiv). Eclogae geol. Helv. 11/4, 484–496.

UNRUH, C.H. and KATZ, D.L. (1949): Gas hydrates of carbon dioxide-methane mixtures. J. Petroleum. Techn. 1, 83–86.

WALTHER, J. (1981): Fluide Einschlüsse im Apatit des Carbonatits vom Kaiserstuhl, Oberrheingraben. Diss. Univ. Karlsruhe.

WEAST, R.C. (1980): CRC Handbook of Chemistry and Physics. 60th edition, CRC press, Boca Raton, Florida.

WIEBE, R. and GADDY, V.L. (1940): The solubility of carbon dioxide in water at various temperatures from 12 to 40° and at pressures to 500 atmospheres. Amer. Chem. Soc. J. 62, 815–817.

ZEMANN, J., ZOBETZ, E., HEGER, G. and VOELENKLE, H. (1979): Strukturbestimmung eines OH-reichen Topases. Anz. (österr.) Akad. Wiss. Wien 6.

Manuscript received April 4, 1987; revised manuscript accepted August 2, 1988.